J Neurophysiol 120: 1293–1306, 2018.
First published May 16, 2018; doi:10.1152/jn.00707.2017.

RESEARCH ARTICLE | *Control of Movement*

Distinct mechanisms explain the control of reach speed planning: evidence from a race model framework

Prasanna Venkhatesh Venkataratamani and Aditya Murthy
Center for Neuroscience, Indian Institute of Science, Bangalore, India

Submitted 1 October 2017; accepted in final form 15 May 2018

Venkataratamani PV, Murthy A. Distinct mechanisms explain the control of reach speed planning: evidence from a race model framework. *J Neurophysiol* 120: 1293–1306, 2018. First published May 16, 2018; doi:10.1152/jn.00707.2017.—Previous studies have investigated the computational architecture underlying the voluntary control of reach movements that demands a change in position or direction of movement planning. Here we used a novel task in which subjects had to either increase or decrease the movement speed according to a change in target color that occurred randomly during a trial. The applicability of different race models to such a speed redirect task was assessed. We found that the predictions of an independent race model that instantiated an abort-and-replan strategy was consistent with all aspects of performance in the fast-to-slow speed condition. The results from modeling indicated a peculiar asymmetry, in that although the fast-to-slow speed change required inhibition, none of the standard race models was able to explain how movements changed from slow to fast speeds. Interestingly, a weighted averaging model that simulated the gradual merging of two kinematic plans explained behavior in the slow-to-fast speed task. In summary, our work shows how a race model framework can provide an understanding of how the brain controls different aspects of reach movement planning and help distinguish between an abort-and-replan strategy and merging of plans.

NEW & NOTEWORTHY For the first time, a race model framework was used to understand how reach speeds are modified. We provide evidence that a fast-to-slow speed change required aborting the current plan and a complete respecification of a new plan, while none of the race models was able to explain an instructed increase of hand movement speed, which was instead accomplished by a merging of a new kinematic plan with the existing kinematic plan.

kinematic planning; movement control; race models; reach movements; speed redirect

INTRODUCTION

A number of psychophysical studies highlight the notion that movement attributes and plans are likely to be represented/programmed in the central nervous system well before execution (Dick et al. 1986; Keele 1968; Morris et al. 1994; Rosenbaum 1985; Summers and Anson 2009). These studies have motivated the use of feedforward computational models containing a complete specification of a movement plan, i.e., where, when, and how a movement is planned before its implementation (Desmurget and Grafton 2000; Wolpert et al. 1995; Wolpert and Ghahramani 2000; Wolpert and Kawato 1998). However, other models suggest that only certain critical features of the movement need to be specified in advance (Desmurget and Grafton 2003; Scott 2004; Todorov and Jordan 2002); hence, the neural representation specifying movements may only be generated dynamically in real time during movement execution. Thus the extent to which the nervous system predetermines the kinematics and dynamics of impending movements is still a matter of debate.

Although an explicit neural representation of movement kinematics has not been described, studies have provided evidence that kinematic parameters like velocity are multiplexed with other information before motor execution. For example, Moran and Schwartz (1999) recorded the activity of the cells in motor and premotor cortex in response to changes in the speed of arm movements and showed that a model with independent (speed only) and interactive (speed and direction) terms described a large portion of motor cortical activity. In separate work, Padoa-Schioppa et al. (2002) found neuronal correlates of kinematics-to-dynamics transformation in the supplementary motor area of two monkeys during the planning phase of visually instructed reaching movements; and more recent work suggests an explicit representation of the kinematic variables such as position and speed of movement in the preparatory activity motor cortical neurons (Churchland et al. 2006; Cisek 2006). In addition to neurophysiological evidence, behavioral and computational evidence also suggests that a kinematic plan can be formed independent of dynamic conditions (Flanagan et al. 1999; Krakauer et al. 1999; Shadmehr and Mussa-Ivaldi 1994). Taken together, these reports suggest the existence of distinct kinematic representations in the brain that constitute an important aspect of motor planning. If distinct kinematic representation such as speed can be planned, it stands to reason that such a variable must also be amenable to voluntary control. To the best of our knowledge, no study has formally tested such a corollary hypothesis. Using a modification of a reach redirect task in which subjects were instructed to change the speed of their movement plan, we assessed the applicability of different race model architectures to explain performance, analogous to the classic redirect task that involves a change in the location of the target (Venkataramani et al. 2018).

Address for reprint requests and other correspondence: A. Murthy, Center for Neuroscience, Indian Inst. of Science, Bangalore 560012, Karnataka, India (e-mail: adi@iisc.ernet.in).

METHODS

Participants

Ten healthy human volunteers (5 men, 5 women) aged between 22 and 28 yr with normal or corrected-to-normal vision participated in two types of speed redirect tasks. All participants were right-handed, and handedness was determined by the score in the Edinburgh Handedness Inventory (Oldfield 1971). Subjects gave written informed consent as per the instructions of the Institute Human Ethics Committee of the Indian Institute of Science, Bengaluru, which approved the protocol. None of the participants knew the purpose of the experiment. Both verbal and written instructions were given before participants performed the behavioral task. For every correct trial, subjects were rewarded monetarily to keep them motivated to do the task.

Experimental Setup

The experimental setup and the recording procedures were same as described in previously published papers from our laboratory (Gopal and Murthy 2015; Jana et al. 2017; Venkataramani et al. 2018). Briefly, visual stimuli were displayed and behavioral parameters were stored with TEMPO/VIDEOSYNC software (Reflective Computing, St. Louis, MO). Hand movements were recorded with an electromagnetic tracking and orienting device (Polhemus LIBERTY, Colchester, VT) at 240 Hz. Visual feedback of the hand was given by a small LED placed at the tip of the index finger. All recordings were performed in a dark room.

Speed Redirect Task

Subjects performed a novel redirect task called the speed redirect task in which they were asked to change the speed of their movements when there was a change in target color. Two separate experiments were conducted, one with a fast-to-slow (FS) redirect condition and the other with a slow-to-fast (SF) redirect condition. The task contained two types of trials, viz., no-switch trials (60%) and switch trials (40%), randomly interleaved. Unlike the classic redirect task, in this task there was only a change in the target color, not the position. Each trial began with a gray fixation box that appeared at the center of the screen for a period of 300–700 ms, and subjects were asked to fixate with their finger on the fixation spot. Targets were presented on a black background of 0.01 cd/m^2 luminance in one of the four cardinal directions with an eccentricity of 12° from the fixation spot. In a switch trial, a change in the color of the target served as a cue to change the speed of the movement.

In the FS experiment, a single green target during no-switch trials [1° × 1°; Commission International de l'Eclairage (CIE) coordinates: $x = 0.299$, $y = 0.494$; luminance: 26 cd/m^2] instructed a fast movement (movement duration ≤200 ms). In the switch trial of this task, the target color changed from green to red (1° × 1°; CIE coordinates: $x = 0.473$, $y = 0.321$; luminance: 25 cd/m^2), instructing subjects to change their planned fast movement into a slow movement (FS; a low movement duration of 500–1,000 ms; Fig. 1*A*) Similarly, in the SF experiment a single red target during no-switch trials instructed a slow movement (duration of 500–1,000 ms). In switch trials, the target color switched from red to green, instructing subjects to change their planned slow movement into a fast movement (SF; a fast movement duration being ≤200 ms; Fig. 1*A*) The time of the color change relative to the first color, called color switch delay (CSD), was chosen randomly from a prescribed set of values (33, 83, 133, 183, 233, 283, 334, 384 ms). Subjects were given auditory feedback on successful trials when they changed their speed plans appropriately. Hand movement beginning and end were marked online based on the electronic window in TEMPO. Online movement duration was defined as the temporal difference between the beginning and end of the movement. All subjects performed ~100 practice trials before each experiment, and subjects performed ~600 trials per session, with a 3-min break after 300 trials. A typical session lasted ~1 h, and the task conditions were counterbalanced across participants.

Compensation Function

In the FS experiment, a correct response for a switch trial was one in which the subject made a slow response from the beginning and reached the target with a movement duration ranging from 500 to 1,000 ms. Switch trials in which the movement duration was <500 ms were marked as erroneous. Similarly, in switch trials of the SF experiment, responses were classified as correct when the subject made a response with a movement duration <200 ms. On the basis of the above-mentioned criterion, a compensation function [$W(t)$] was constructed by plotting the probability of an erroneous response as a function of CSD for both tasks. Construction of the compensation function assessed the behavioral performance during speed redirection. As in the classic redirect task, as the CSD becomes progressively longer it becomes harder to change kinematic plans, resulting in more errors at longer CSD. Plots were superimposed with the best-fit cumulative Weibull function to quantify a subject's performance (see Fig. 2):

$$W(t) = \gamma - (\gamma - \delta) \times \exp\left[-(t/\alpha)^{\beta}\right]$$

where t is the time, α is the time at which the function reaches 64% of its full growth, β is the slope, γ is the maximum value of the function, and δ is the minimum value of the function. One way to evaluate the performance of subjects was to check whether ($\gamma - \delta$) was >0.5; for all subjects it was >0.5 (Bhutani et al. 2012). Thus subjects did not employ any other covert strategy such as delaying their primary response to produce correct responses.

Analyses

All off-line analysis and statistical tests were performed with MATLAB (MathWorks, Natick, MA). Trials in which the reaction time (RT) was >700 ms and having a movement duration >1,000 ms were not included in the analysis. Hand movement beginning and end were marked when 10% of the peak velocity was reached for all the movements in both experimental conditions and was subsequently verified manually with a custom-made graphical user interface (GUI). The accuracy of hand movement detection was subsequently manually verified for every trial with a GUI in MATLAB developed in the laboratory. All data were first checked for normality with a Lilliefors test. If this was satisfied, a two-tailed t-test was used along with Cohen's d to measure the size effect; otherwise a signed-rank test was used. One-way ANOVAs were performed and reported along with partial η^2 (η_p^2) to measure the effect size. Unless otherwise mentioned, the level of significance (α) was fixed at 0.05. Claims on the null hypothesis were based on the Bayes factor (BF_{10}), which measures the ratio of the likelihood of the alternate or null being true given the data. If BF_{10} was <0.3 then H_0 was accepted. To determine the unimodality of the distribution, Hartigan's dip statistics were used. The best model was selected based on multiple criteria. First, the model's ability to predict the Weibull mean at the population level was checked, followed by its ability to predict the cumulative distribution function (CDF) of the experimental Weibull function, which was tested individually for each subject by Kolmogorov-Smirnov (KS) test. A binomial test was performed to find the significance over the number of individuals who passed the KS test mentioned above. In addition to the above, the predicted and observed mean error response were tested on a population level and at the individual level for the same model. If the model passed all the above tests, the model's ability to predict the fanning effect was finally used to confirm the model.

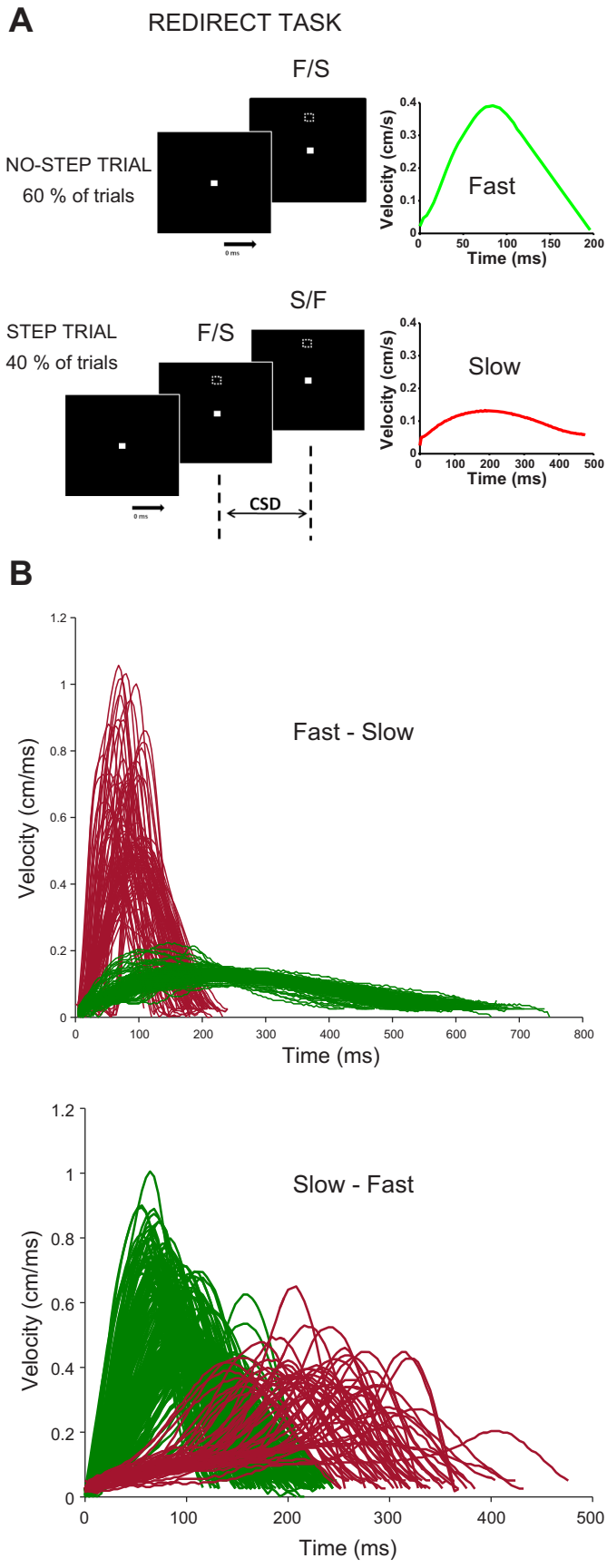

Modeling RT Distributions

A modified drift-diffusion framework was used to model the RT distribution. This model is essentially a competitive accumulation to threshold model, adapting some characteristics of the drift-diffusion model like within-trial variability and interaction with competing accumulators, respectively (Usher and McClelland 2001). According to this framework, the evolving motor plan can be abstracted as an accumulator. Computationally, such preparatory activity before a movement is represented by a "GO" unit that starts after a visual delay of 60 ms following stimulus presentation. After a fixed threshold is reached, the movement is initiated. The stochastic equation that was used for modeling the preparatory activity is given below:

$$a_{GO}(t) = a_{GO}(t-1) + \mu_{GO} + \xi_{GO} \quad (1)$$

where $a_{GO}(t)$ represents the current level of GO unit activation at time step t. The mean growth rate of the GO unit is given by μ_{GO}. ξ_{GO} is a Gaussian noise term that represents the noise in the input signal, which has a zero mean and a standard deviation.

Modeling Performance

Eight different computational models were identified that can explain performance in a speed redirect task.

GO-GO models. Three GO-GO models were designed to explain speed redirect behavior. Since GO1 represents the fast movement plan and GO2 represents the slow movement plan in a FS task and vice versa for the SF task, the rates at which these two units accumulate were considered to be different, as the corresponding RTs for slow and fast movements were also different. The race between these two units determined the outcome of a given trial. Different GO-GO models are distinguished by the kind of interactions between the GO processes. The three GO-GO models are described by the following equations:

$$a_{GO1}(t) = a_{GO1}(t-1) + \mu_{GO1} - \beta_{GO2} \times a_{GO2}(t-1) + \xi_{GO1} \quad (2)$$

$$a_{GO2}(t) = a_{GO2}(t-1) + \mu_{GO2} - \beta_{GO1} \times a_{GO1}(t-1) + \xi_{GO2} \quad (3)$$

where GO1 and GO2 are the two accumulator units instantiating the GO process with different rates, β_{GO2} is the coefficient of the inhibitory interaction of GO2 on GO1, and β_{GO1} represents the interaction of GO1 on GO2. The three models are GO-GO independent (GG-i; when $\beta_{GO1} = \beta_{GO2} = 0$), GO-GO with symmetric interaction (GG-s; when $\beta_{GO1} = \beta_{GO2} \neq 0$), and GO-GO with asymmetric interaction (GG-a; when $\beta_{GO1} \neq \beta_{GO2}$).

GO-STOP-GO models. Five GO-STOP-GO models were simulated with the equations given below:

$$a_{GO1}(t) = a_{GO1}(t-1) + \mu_{GO1} - \beta_{GO1} \times a_{STOP}(t-1) + \xi_{GO1} \quad (4)$$

$$a_{GO2}(t) = a_{GO2}(t-1) + \mu_{GO2} - \beta_{GO2} \times a_{STOP}(t-1) + \xi_{GO2} \quad (5)$$

$$a_{STOP}(t) = a_{STOP}(t-1) + \mu_{STOP} + \xi_{STOP} \quad (6)$$

$$a_{GO}(t) = a_{GO}(t-1) + \mu_{GO} - \beta_{STOP} \times a_{STOP}(t-1) + \xi_{GO} \quad (7)$$

$$a_{STOP}(t) = a_{STOP}(t-1) + \mu_{STOP} - \beta_{GO} \times a_{GO}(t-1) + \xi_{STOP} \quad (8)$$

Fig. 1. Illustration of the temporal sequence of stimuli in redirect task. *A*: temporal sequence of events in a speed redirect task. No-switch trials display a single target (shown as a dotted box), green [in the fast-to-slow (FS) task] or red [in the slow-to-fast (SF) task], after a fixation time in a random 60% of the trials. In a switch trial, the green target changed its color to red after a variable color switch delay (CSD), indicating the need to decrease the speed of the movement in the FS task and vice versa in the SF task. The response to a green target is a speeded movement, and the velocity profile is shown in green. The response to the red target is a slow movement, and the representative velocity profile is shown in red. *B*: velocity traces of all switch trials in the speed redirect task of an exemplar subject. *Top*: FS task. *Bottom*: SF task. Green traces are correct trials; red traces are incorrect trials.

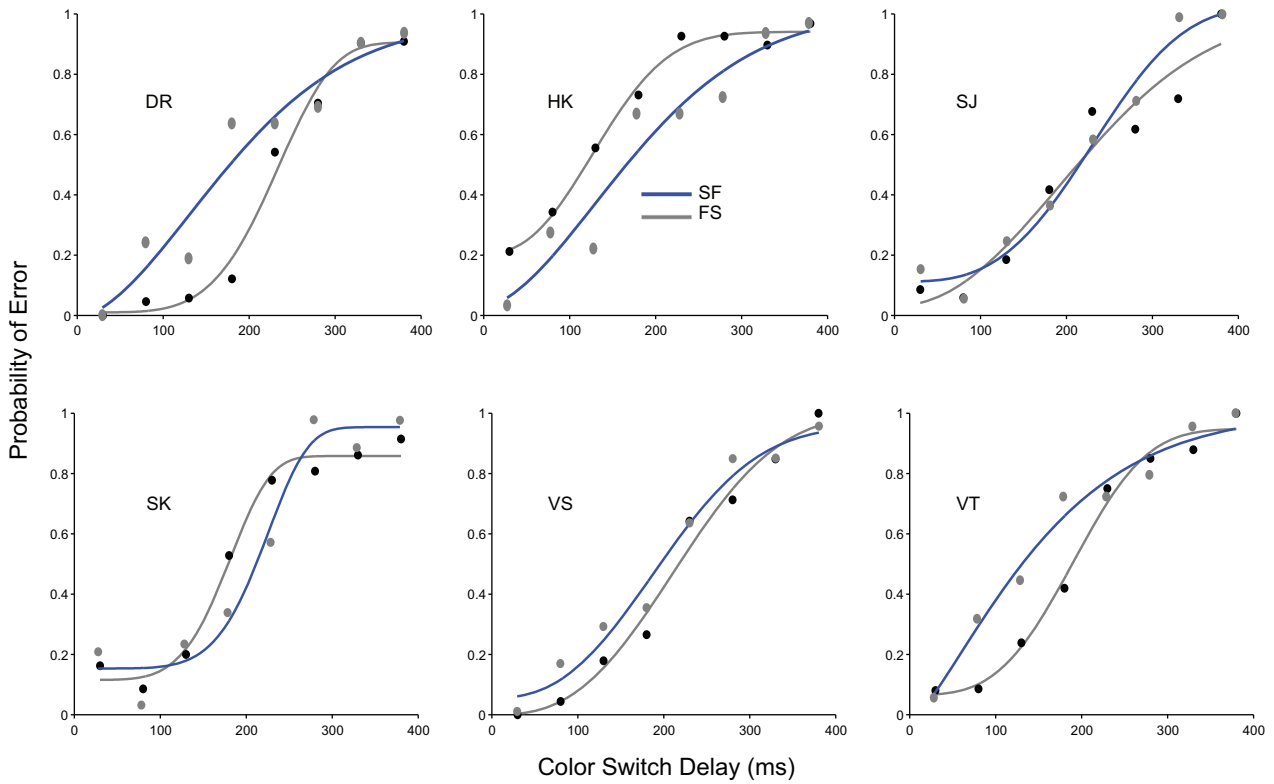

Fig. 2. Compensation functions of the fast-to-slow (FS) and slow-to-fast (SF) speed redirect tasks: plots showing the probability of making an erroneous fast hand movement to the target as a function of color switch delay (CSD) for the FS task and a slow hand movement to the target as a function of CSD for the SF task. Data for 6 exemplar subjects (*subjects DR*, *HK*, *SJ*, *SK*, *VS*, *VT*) are shown superimposed with a best-fit cumulative Weibull function indicating that the probability of making an erroneous movement to the target increased with CSD.

GO-STOP-GO (or equivalently GO-GO-STOP) independent, GO-STOP-GO symmetric, GO-STOP-GO asymmetric, and GO-STOP-GO asymmetric 2 were the four models that were simulated. A mutually interacting GO-STOP model was also tested, as described by Boucher et al. (2007).

Model Implementation

The model implementation is described in detail elsewhere in previously published work (Gopal and Murthy 2016; Ramakrishnan et al. 2012; Venkataramani et al. 2018). Briefly, the parameters that characterize the GO processes (μ_{GO}, σ_{GO}) were estimated with a Monte Carlo method. The least squares error (LSE) between the observed and simulated no-switch RT distributions was minimized in the parameter space with a nonlinear minimization procedure (FMINCON in MATLAB), which ran 1,000 iterations. Different sets of initial parameters were used so as to avoid convergence to suboptimal solutions. The parameter set (μ_{GO}, σ_{GO}) that resulted in the smallest value of the LSE was chosen as the optimal solution. In the FS task, the parameters of the GO1 and GO2 units were obtained from the no-switch RT distributions of the FS and SF tasks, respectively. In the SF task the parameters of the GO1 and GO2 units were obtained from the no-switch RT distributions of the SF and FS tasks, respectively. In the GO-GO models, along with single GO1 processes, another GO2 was simulated that began to accumulate after the appearance of the second target. When the GO1 process reached the threshold first, the response to the first target (slow or fast) was considered initiated; when the GO2 process reached the threshold first, a correct response to the second target (fast or slow) was initiated. Five hundred switch trials were simulated for each CSD, and the fraction of erroneous trials in each CSD was calculated. The LSE between the simulated and the observed compensation function was minimized in the parameter space to estimate the optimal values for the parameters depending on the model.

LATER Model Simulations

The LATER (linear approach to threshold with ergodic rate; Carpenter and Williams 1995) model has been successful in explaining the RTs of saccadic and reach movements. The model assumes that the GO and STOP processes are stochastic and independent of each other and the rate at which these processes vary can be described by a Gaussian distribution (Hanes and Carpenter 1999; Hanes and Schall 1996; Ramakrishnan et al. 2010; Reddi et al. 2003). Monte-Carlo simulations were run with MATLAB to estimate the rates of the GO and the STOP processes as described previously in Ramakrishnan et al. (2010). The reprocessing time (RPT) values were simulated with a LATER model framework, in which the activity ramps to a threshold.

On a no-switch trial, the rate of the GO process starts after a visual delay of 60 ms from the presentation of the target. This was randomly chosen from a Gaussian distribution with mean μ_{go} and standard deviation σ_{go} and accumulates to a threshold that is taken as unity. Once the GO process reached the threshold, a movement to the presented target was assumed to have been elicited. The μ_{go} and σ_{go} were estimated by simulating 2,000 no-switch trials. A KS statistic was used to compare the simulated cumulative distribution with that of the experimental distribution. The difference in the KS statistic between the simulated and the observed data was minimized in the parameter space with a nonlinear minimization procedure in MATLAB, and convergence was decided based on the minimal error in the KS statistic between the observed and the simulated data (Reddi and Carpenter 2000). Different sets of initial and final parameter values were used so as to avoid convergence to a local minimum before choosing the best parameter values. The whole procedure was repeated 200 times for

each subject. On switch trials, the GO process was initiated 60 ms after the initial target, using the no-switch trials parameters (μ_{go}, σ_{go}). For each trial, the CSD was chosen randomly from the set of CSDs used in the experiment. The time at which the activity reached threshold was the RT. The RPT for each trial was the time interval between the onset of the target switch and the first saccade RT, which was given by *Eq. 9*:

$$RPT_{sim} = RT_{GO} - CSD \quad (9)$$

RESULTS

Speed Redirect Task

Behavioral data were collected from 10 subjects on both the FS and SF speed redirect tasks. The performance of subjects in the speed redirect task was assessed by plotting the probability of an erroneous response as a function of CSD on switch trials. As expected, the probability of error increased with increasing CSD in all subjects in both tasks. A Weibull function was fit to the performance of each subject. The Weibull fit parameters were calculated for both the FS and SF speed redirect tasks. [FS Weibull fit parameters: range ($\gamma - \delta$): min = 0.91, max = 1, median = 0.9579; slope (β): min = 1.9, max = 5.07, median = 3.3; SF Weibull fit parameters: range ($\gamma - \delta$): min = 0.902, max = 1, median = 0.94402; slope (β): min = 1.92, max = 3.77, median = 2.44]. In general, subjects were able to do the task well, and the behavior conformed to the performance curves seen in the standard redirect task (Venkataramani et al. 2018).

In the FS task, the movement duration (MD; 132 ± 6.6 ms; min = 94 ms; max = 156 ms) and the peak velocity (PV; 330 ± 40 cm/s; min = 185 cm/s; max = 515 cm/s) in no-switch trials were significantly different (MD: $t = -7.35$, df = 9, $P < 0.001$, $d = 1.85$, PV: $t = 5.29$, df = 9, $P < 0.001$, $d = 2.3$) from switch correct trial movement durations (528 ± 5.4 ms; min = 623 ms; max = 677 ms) and peak velocity (149 ± 1.7 cm/s; min = 62 cm/s; max = 239 cm/s). All subjects showed significance for both movement duration and peak velocity between the no-switch trials and switch correct trials (10/10; MD, $P < 0.001$; PV, $P < 0.001$). Similarly, in the SF task, the movement duration in no-switch trials (MD: 536 ± 33 ms; min = 457 ms; max = 675 ms) and the peak velocity (97 ± 11 cm/s; min = 47 cm/s; max = 147 cm/s) were also significantly different from switch correct movement durations (140 ± 8.8 ms; min = 116 ms; max = 201 ms; $t = 10.803$, df = 9, $P < 0.001$, $d = 5.6$) and peak velocity (197 ± 15 cm/s; min = 136 cm/s; max = 283 cm/s; $t = -4.86$, df = 9, $P < 0.001$, $d = 2.32$). Figure 1*B* shows the velocity traces of all the switch trials for the FS and SF tasks for an exemplar subject. Interestingly, two distinct clusters of velocity traces were found in the FS task that corresponded to the durations instructed for slow and fast movements but were not observed in the SF task (represented in Fig. 1*B*). These distinct sets of patterns were further analyzed and are presented in Fig. 8, where the movement duration is plotted as a function of RPT. Individual subjects (10/10; MD: $P < 0.05$; PV: $P < 0.001$) also showed the same trend as the population data. These results indicate that the subjects did the task as per the instructions. Additionally, the RTs of the fast no-switch trials (415 ± 13 ms) in the FS task were consistently and significantly different from the RTs of the slow no-switch trials (477 ± 21 ms) in the SF task. Ten of ten subjects showed a significant difference (*t*-test; $P < 0.05$) between the RTs of fast and slow no-switch trials.

Testing Race Models of Redirect Performance

To describe the computational mechanisms underlying the performance of the speed redirect tasks (both FS and SF), various race models were tested. The GO-GO and GO-STOP-GO models were tested to check whether they could explain the performance of subjects and were used to compare the results of the computational architectures between the FS and SF tasks.

GO-GO models. In the GO-GO model, performance is determined by the outcome of the race between two independent GO1 and GO2 processes. In the FS task, GO1 and GO2 represent two distinct plans, and a race can be conceived between the accumulator that represents the fast movement and another accumulator that represents the slow movement. Since the RTs in the fast and slow no-switch trials were significantly different from each other, the rates of the GO1 and GO2 units were considered different in all the GO-GO models. For the FS task, the GO1 and GO2 rates were obtained from the no-switch trials of the FS and SF tasks, which were fast and slow movements, respectively. The rates of the GO units in the SF task were likewise obtained from the no-switch trials of the SF and FS tasks, respectively.

In the GO-GO independent model, the interaction terms were kept to zero. In the speed task, the target did not jump to a new position; only the color of the target changed, and the outcome of the race was either a slow movement or a fast movement depending on the task. In the model simulations of the FS task, if the GO1 process reached threshold first, a fast movement (erroneous response) was initiated; otherwise a slow movement was initiated (correct response). Similarly, in the model simulations of the SF task, if the GO1 process reached the threshold first, a slow movement was initiated (error response) and if the GO2 process reached the threshold first a fast movement was made (correct response). A compensation function was constructed for the GO-GO independent model for both tasks based on the simulations. The results of the simulations were quantified by the ability of the model to predict the Weibull mean of the compensation function across the population.

The experimental and simulated compensation functions are shown in Fig. 3, *A* and *C*, for all the GO-GO models. The predicted and observed Weibull means were significantly different from each other [FS: $t = 7.6170$, df = 9, $P < 0.001$, $d = 3.49$ (Fig. 4*A*); SF: $t = 10.732$, df = 9, $P < 0.001$, $d = 3.89$ (Fig. 4*D*)]. All subjects (10/10) showed a significant difference in the KS test between the simulated and observed Weibull fitted CDFs, with $P < 0.05$ for both FS and SF tasks. Apart from predicting the compensation function, race models can also predict the RTs of the erroneous responses in a switch trial. The predicted mean erroneous response RTs were significantly different from the experimental data for the FS task and were significantly different at the population level for the FS task but not the SF task (FS: $t = -4.7537$, df = 9, $P = 0.001$, $d = 0.34$; SF: $t = -0.8605$, df = 9, $P = 0.4119$, d = 0.08, $BF_{10} = 0.4198$). Moreover, 8/10 subjects for the FS task and 7/10 subjects for the SF task showed a significant difference in

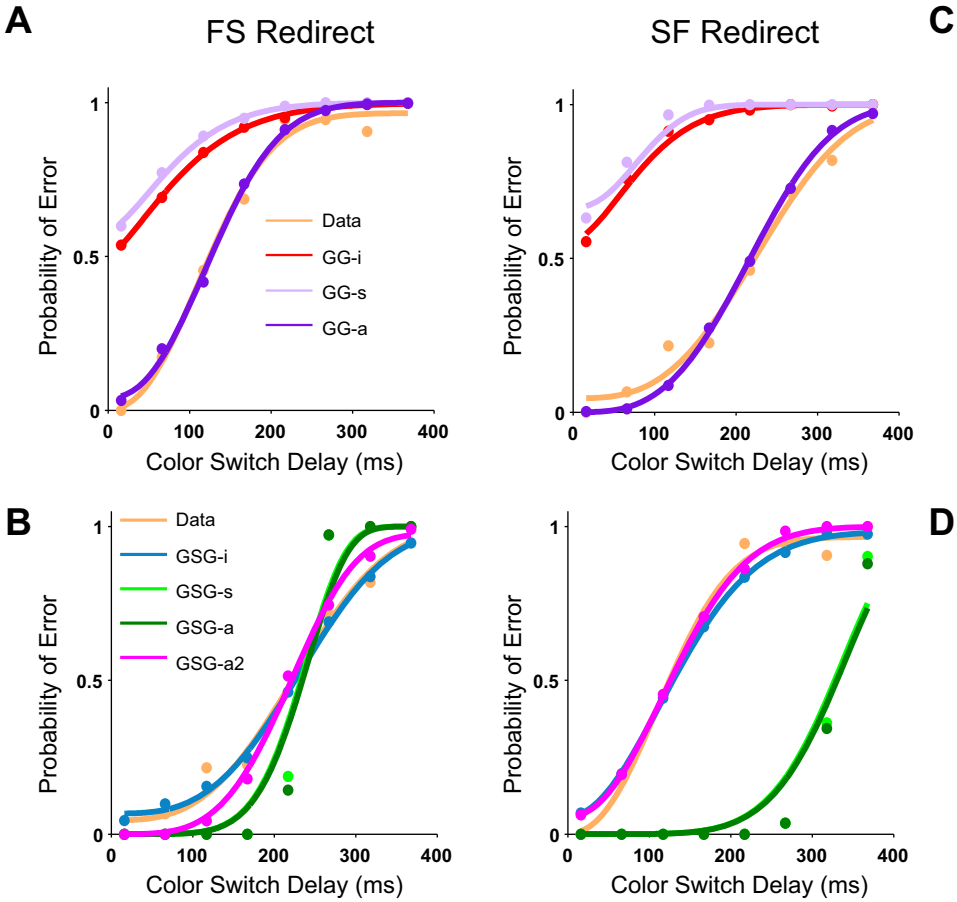

Fig. 3. Simulation results of the GO-GO and GO-STOP model architectures for fast-to-slow (FS) and slow-to-fast (SF) tasks. *A* and *C*: the compensation function generated by the 3 GO-GO models for a single subject shown in different colors along with the actual data for the FS and SF redirect tasks, respectively. *B* and *D*: the compensation function generated by the 4 GO-STOP-GO models for a single subject shown in different colors along with the actual data for the FS and SF redirect tasks, respectively. GG-i, GG-s, GG-a, GO-GO-independent, -symmetric, and -asymmetric models; GSG-i, GSG-s, GSG-a, GSG-a2, GO-STOP-GO-independent, -symmetric, -asymmetric, and -asymmetric 2 models.

the KS test, with $P < 0.05$ when the simulated error distributions were directly compared to that of the observed error distribution.

The interactions between the GO units were made mutually inhibitory (GG-s; $\beta_{GO1} = \beta_{GO2}$) or asymmetric (GG-a; $\beta_{GO1} \neq \beta_{GO2}$) to overcome the shortcomings of the independent model. Simulations were performed to optimize the value of the coefficient of inhibition in these models. The GG-s model failed to predict the Weibull mean for both tasks [FS: $t = 7.9794$, df $= 9$, $P < 0.001$, $d = 3.6$ (Fig. 4*B*); SF: $t = 10.407$, df $= 9$, $P < 0.001$, $d = 3.5$ (Fig. 4*E*)]. In both tasks (FS and SF) all 10 subjects showed a significant difference in the KS test between the simulated and observed Weibull fitted CDFs, with $P < 0.05$. The symmetric model also failed to explain the RT of the erroneous response for the FS task, but for the SF task, the predicted and observed erroneous RTs were not significantly different from each other (FS: $t = -7.271$, df $= 9$, $P < 0.001$, $d = 0.68$; SF: $t = -1.7641$, df $= 9$, $P = 0.115$, $d = 0.22$, $BF_{10} = 0.9758$). All subjects (10/10) in the FS task and 7/10 subjects in the SF task showed a significant difference between the observed and simulated error response RTs in the KS test, with $P < 0.05$.

The major shortcoming of this model was that the GO2 process, which started later in the race, had a disadvantage in overcoming the inhibitory interaction of the GO1 unit; as a result, the GO1 process won the race most often. Thus a GO-GO asymmetric model was tested to see whether it could capture the performance of subjects in the speed redirect tasks. The predictions of the asymmetric model were not significantly different from the observed Weibull means of the compensation function for both tasks [FS: $t = 0.1091$, df $= 9$, $P = 0.9155$, $d = 0$, $BF_{10} = 0.3104$ (Fig. 4*C*); SF: $t = 0.366$, df $= 9$, $P = 0.7228$, $d = 0.14$, $BF_{10} = 0.3271$ (Fig. 4*F*)]. Nine of ten subjects in the FS task and eight of ten subjects in the SF task showed no significant difference in the KS test between the simulated and observed Weibull fit CDFs, with $P > 0.05$. However, the model failed to explain the RT of the erroneous response in both tasks (FS: $t = -12.15$, df $= 9$, $P < 0.001$, $d = 1.32$; SF: $t = -9.8045$, df $= 9$, $P < 0.001$, $d = 2.23$). All subjects (10/10) in both tasks showed a significant difference between the experimental and predicted error response RTs in the KS test, with $P < 0.05$.

GO-STOP-GO models. In these models, apart from the two GO units, a STOP unit was also introduced. Since the FS task requires subjects to deliberately slow down their responses while executing fast movements, a STOP process might explain the behavior of the FS task. Five GO-STOP-GO models were tested as mentioned in METHODS. First among the GO-STOP-GO models assessed was the GO-STOP-GO independent models in which the GO and STOP units accumulate independently to a threshold. Simulations were executed to optimize the STOP parameters (μ_{STOP}, σ_{STOP}) to fit the predicted and experimental compensation functions. As expected, the predicted and experimental Weibull means of the compensation function were not significantly different for both tasks [FS: $t = 0.0418$, df $= 9$, $P = 0.9675$, $d = 0$ (Fig. 3*B*); SF: $t = 1.824$, df $= 9$, $P = 0.101$, $d = 0.24$ (Fig. 3*D*)]. A Bayes factor analysis of the same showed moderate evidence in support of

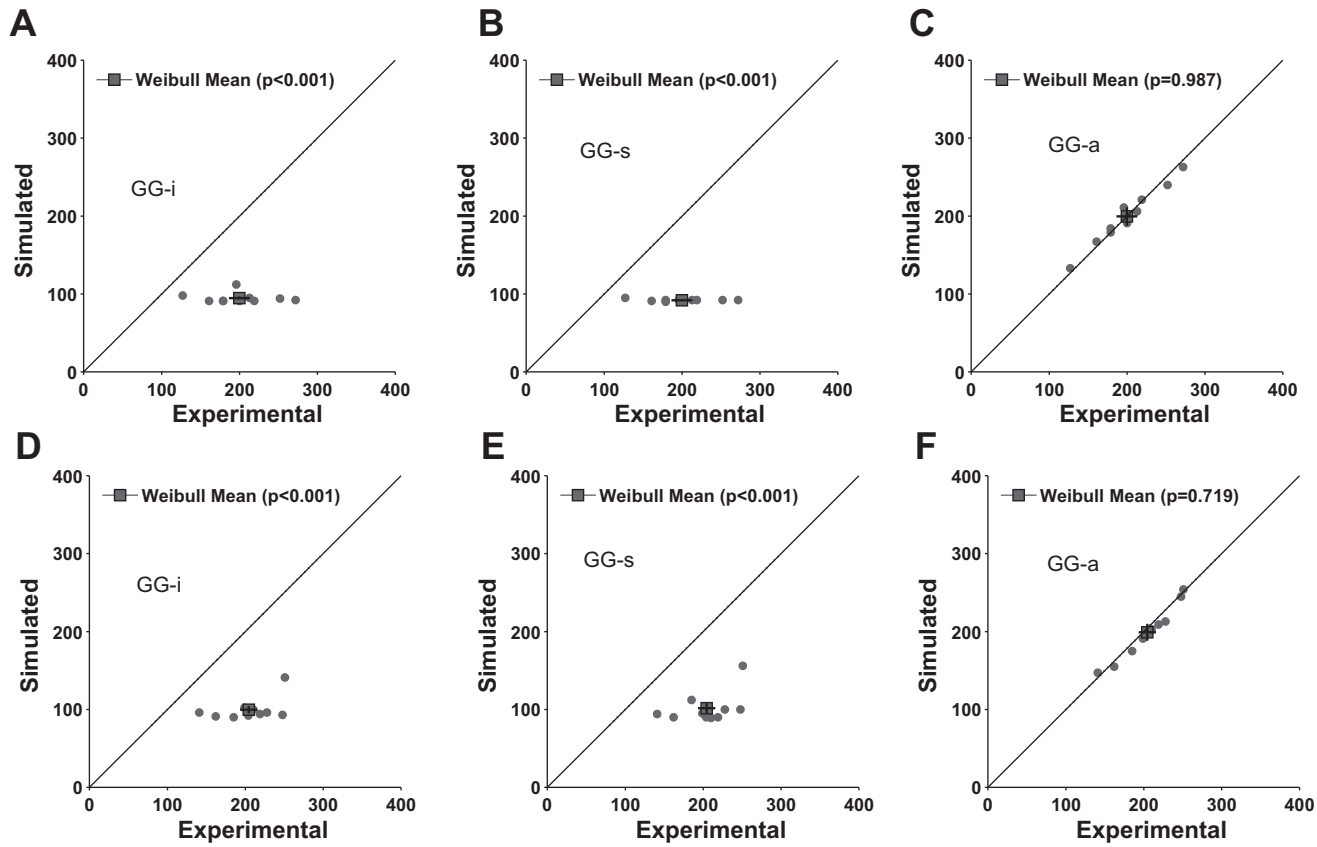

Fig. 4. Testing GO-GO models. Experimental and simulated compensation functions were quantified by calculating the Weibull means and are plotted against each other. *A–C*: the quantification plot for GO-GO-independent (GG-i), symmetric (GG-s), and asymmetric (GG-a) models, respectively, for the fast-to-slow (FS) redirect task. *D–F*: same for the slow-to-fast (SF) redirect task. Each dot represents a subject. Filled squares represent the predicted and observed Weibull means across subjects.

this claim for the FS but not the SF task (FS: $BF_{10} = 0.3091$; SF: $BF_{10} = 1.044$). In addition, 10/10 subjects in the FS task and 7/10 subjects in the SF task showed no significant difference in the KS test between the simulated and observed Weibull fitted CDFs, with $P > 0.05$. No significant difference between the GO-STOP-GO independent model was observed between the predicted and observed RTs of the erroneous response for the FS task, but a significant difference was observed in the SF task (FS: $t = 1.2068$, df = 9, $P = 0.257$, $d = 0.08$, $BF_{10} = 0.5527$; SF: $t = 3.084$, df = 9, $P = 0.01$, $d = 0.388$). Eight of ten subjects in the FS task and six of ten subjects in the SF task did not show significance when the experimental error response RT was compared to the simulated data in the KS test, with $P > 0.05$.

We also tested symmetric and asymmetric versions of the GO-STOP-GO models. The GO-STOP-GO symmetric model was not able to predict the Weibull means for both tasks [FS: $t = -3.02$, df = 9, $P < 0.05$, $d = 1.29$ (Fig. 5*B*); SF: $t = -2.6477$, df = 9, $P < 0.05$, $d = 1.42$ (Fig. 5*F*)]. All subjects (10/10) in both FS and SF tasks showed a significant difference in the KS test between the simulated and observed Weibull fit CDFs, with $P < 0.05$. The fixed asymmetric model was also not able to predict the Weibull means for both tasks [FS: $t = -3.03$, df = 9, $P < 0.05$, $d = 1.31$ (Fig. 5*C*); SF: $t = -2.785$, df = 9, $P < 0.05$, $d = 1.42$ (Fig. 5*G*)]. All subjects (10/10) in both tasks showed a significant difference in the KS test between the simulated and observed Weibull fit CDFs, with $P < 0.05$. Both the symmetric and fixed asymmetric models were also not able to predict error response RTs (Fig. 6). In the symmetric model, 9/10 subjects in the FS task and 10/10 subjects in the SF task showed a significant difference between the observed and predicted error response RTs in the KS test, with $P < 0.05$ (FS: $t = -5.2827$, df = 9, $P < 0.05$, $d = 0.839$; SF: $t = -8.3281$, df = 9, $P < 0.05$, $d = 0.68$). In the fixed asymmetric model, 9/10 subjects in the FS task and 10/10 subjects in the SF task showed a significant difference between the observed and predicted error response RTs in the KS test, with $P < 0.05$ (FS: $t = -5.2288$, df = 9, $P < 0.05$, $d = 0.89$; SF: $t = -3.0706$, df = 9, $P < 0.05$, $d = 1.42$).

Interestingly, there was no significant difference between the predicted and observed Weibull means of the compensation function in the GO-STOP-GO model with the coefficient of inhibition as a free parameter for both tasks [FS: $t = -1.383$, df = 9, $P = 0.205$, $d = 0.15$, $BF_{10} = 0.6521$ (Fig. 5*D*); SF: $t = 0.1709$, df = 9, $P = 0.8680$, $d = 0.15$, $BF_{10} = 0.3121$ (Fig. 5*H*)]. Eight of ten subjects for the FS task and nine of ten subjects for the SF task showed no significant difference in the KS test between the simulated and observed Weibull fit CDFs, with $P > 0.05$. However, the model failed to explain the error response in the FS task but not the SF task (FS: $t = -4.35$, df = 9, $P < 0.05$, $d = 0.603$; SF: $t = 0.1811$, df = 9, $P = 0.8603$, $d = 0.04$, $BF_{10} = 0.3132$). In the FS task 10/10 subjects showed a significant difference between the experimental and predicted error response RTs in the KS test, with $P < 0.05$.

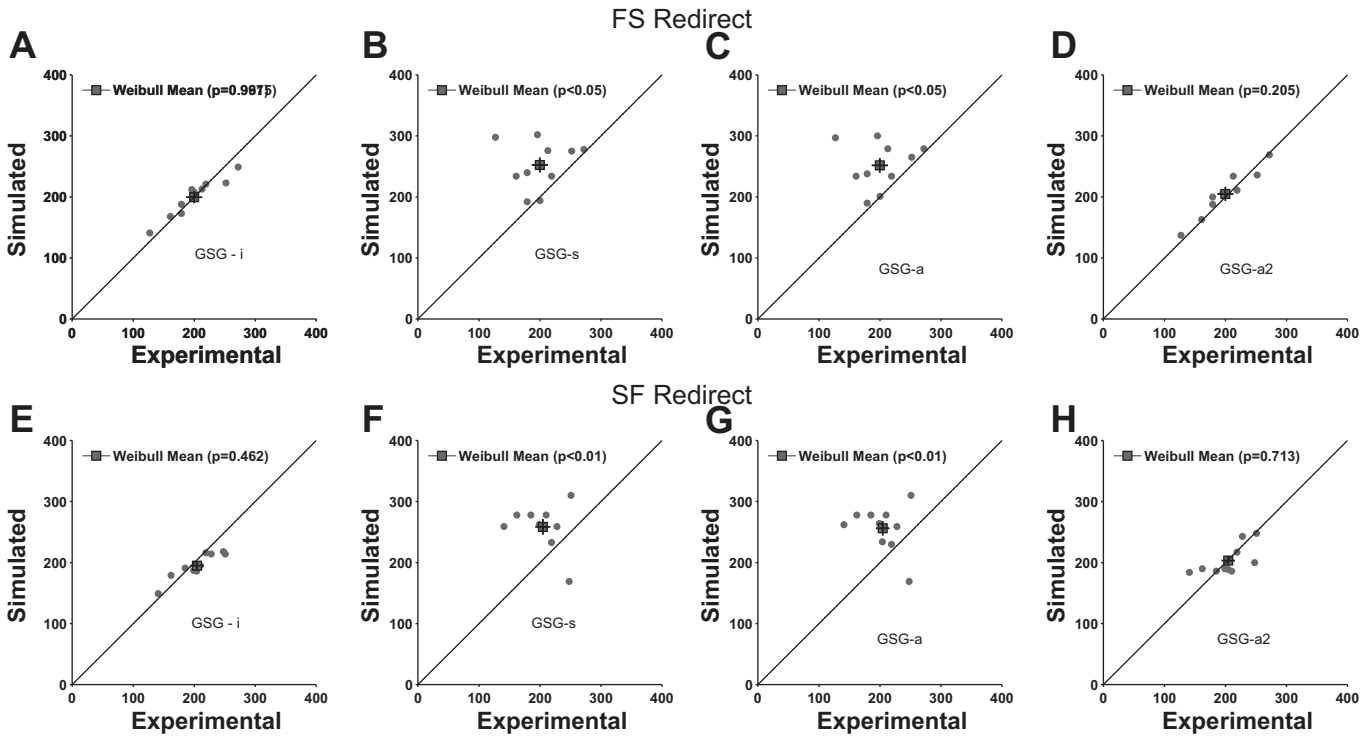

Fig. 5. Testing GO-STOP-GO models. Experimental and simulated compensation functions were quantified by calculating the Weibull means and are plotted against each other. *A–D*: the quantification plot for GO-STOP-GO-independent (GSG-i), -symmetric (GSG-s), -asymmetric (GSG-a), and -asymmetric 2 (GSG-a2) models, respectively, for the fast-to-slow (FS) redirect task. *E–H*: same for the slow-to-fast (SF) redirect task. Each dot represents a subject. Filled squares represent the predicted and observed Weibull means across subjects.

Although the error responses of the SF condition did not show significance at the population level, 7 of 10 subjects showed a significant difference between the experimental and the simulated error RTs in the KS test, with $P < 0.05$.

We also tested a mutually interacting GO-STOP model (see METHODS for details) that showed no statistical difference between the predicted the Weibull means for both FS and SF tasks (FS: $t = -1.237$, df = 9, $P = 0.267$, $d = 0.09$; SF: $t = -0.7894$, df = 9, $P = 0.4503$, $d = 0.05$). Seven of ten subjects in the FS task and nine of ten subjects in the SF task showed no significant difference in KS test between the simulated and observed Weibull fit CDFs, with $P > 0.05$. But this model also failed to explain the error response for both tasks (FS: $t = -4.24$, df = 9, $P < 0.05$, $d = 0.63$; SF: $t = -3.05$, df = 9, $P < 0.05$, $d = 0.68$). In both tasks all subjects showed a significant difference between the experimental and simulated error response RTs in the KS test, with $P < 0.05$.

To summarize, none of the GO-GO or GO-STOP-GO models was able to explain the redirect behavior of the SF task and its erroneous response RTs. In contrast, for the FS task all the models, except for the GO-STOP-GO independent model, could be rejected (see Table 1 for a summary). Taken together, these findings suggest that the GO-STOP-GO independent model was the preferred model to explain performance in the FS task.

Testing Race Model Predictions of the Fanning Effect

If performance in the FS task can be explained by the independent race model, it should show the fanning effect. Conversely, if the SF task is not explained by the GO-STOP-GO independent model, it should fail to show the fanning effect. Briefly, the fanning effect is a consequence of the stochastic independence of the GO and STOP processes, which predicts that the cumulative distribution of the error RT for shorter CSDs will be to the left and will progressively shift rightward (longer RTs) for longer CSDs, approaching the cumulative no-switch RT distribution. This prediction was tested on both the experimental and the simulated data for the FS and SF tasks. The fanning effect was also quantified by taking the difference between the 50th percentile of the cumulative error for every CSD and that of the no-switch RT distribution (Fig. 7*C*). Clearly, in the FS task the experimental data (ANOVA, $F = 2.16$, df = 7, $P < 0.05$, $\eta_p^2 = 0.253$, slope = 111.2; Fig. 7*A*) and the GO-STOP-GO independent model (ANOVA, $F = 8.41$, df = 7, $P < 0.001$, $\eta_p^2 = 0.472$, slope = 64.12) showed evidence of the fanning effect. In contrast, and as expected, all the other models did not show the fanning effect ($P > 0.05$) for the FS task since they possess an interactive term that destroyed the independence assumption. Interestingly, in the SF task the experimental data also did not show any significant evidence of the fanning effect (ANOVA, $F = 0.12$, df = 7, $P = 0.996$, $\eta_p^2 = 0.0145$; Fig. 7*B*), reinforcing why the GO-STOP-GO independent model failed to explain the error RTs of the data (ANOVA, $F = 0.44$, df = 7, $P = 0.8687$, $\eta_p^2 = 0.079$).

Evidence for Merging of Plans in the SF Task

The modeling and performance results thus far showed a contrast between the FS and SF tasks such that FS behavior was better explained by the GO-STOP-GO independent model whereas none of the race models was able to predict the

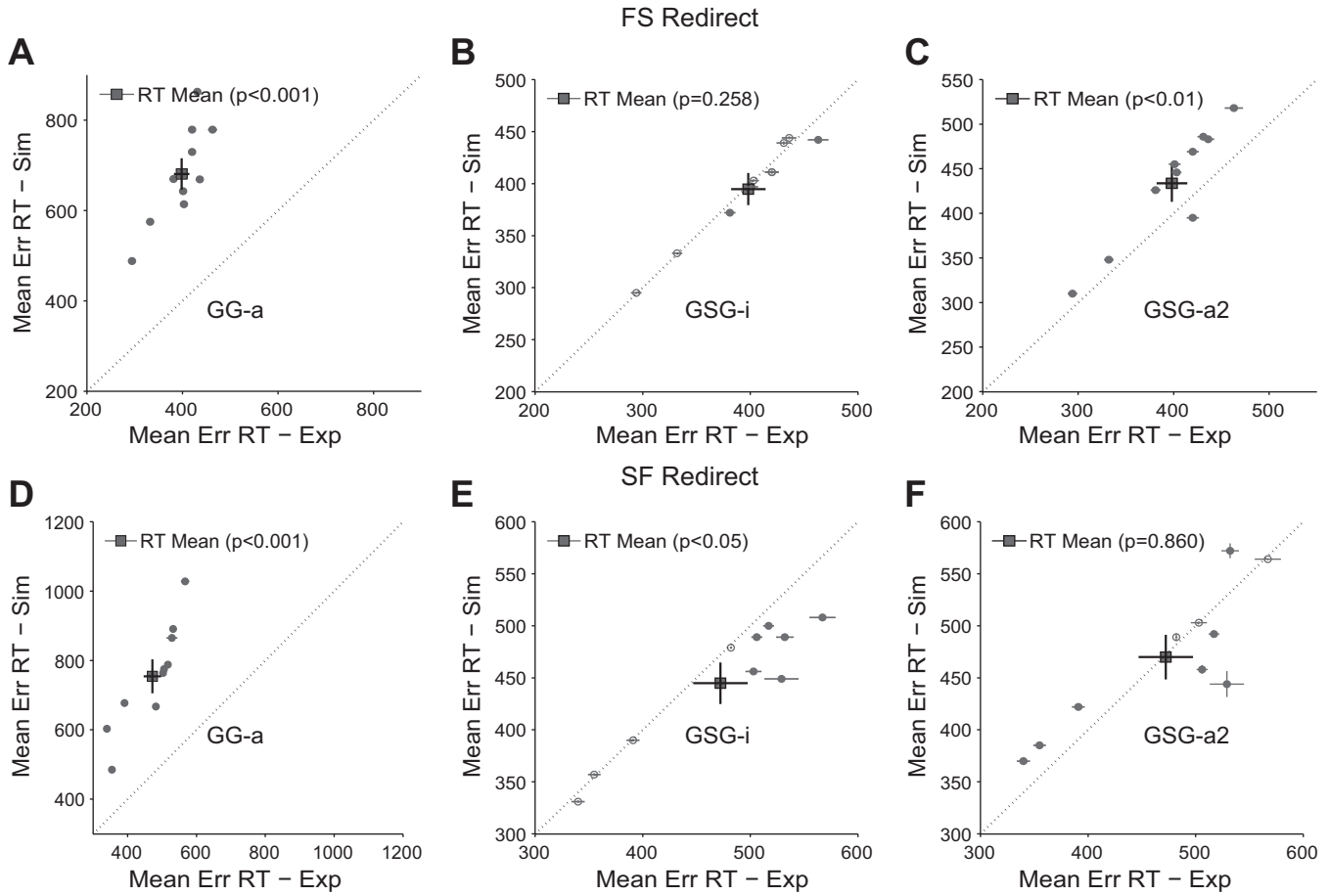

Fig. 6. Prediction of mean error response reaction times (RTs) of the best models. *A–C*: scatterplot of the mean RT of the erroneous responses in switch trials of the experimental data (Exp) with that of the simulated data (Sim) for the GO-GO-asymmetric (GG-a), GO-STOP-GO-independent (GSG-i), and GO-STOP-GO-asymmetric 2 (GSG-a2) models in the fast-to-slow (FS) redirect task. *D–F*: same for the slow-to-fast (SF) redirect task.

behavior in the SF task (see Table 1). This raised the hypothesis that in the FS task there is a stopping mechanism and a new plan initiates the new movement, whereas in the SF task the same plan is being gradually replaced in time with a new plan. This hypothesis can be tested by plotting the movement duration of switch trials as a function of RPT, which is defined as the time interval between the color switch and the reach movement RT. In principle, this is the time that the motor system has to reprogram or reprocess the new instruction to change the movement speed. If there exist two distinct movement plans, then one should expect two distinct distributions of movement durations. On the other hand, if two movement plans gradually merge during a switch trial, one would expect a single distribution of the movement duration. In the FS task, when the movement duration was plotted as a function of RPT it showed a positive trend overall (Pearson's $r = 0.4550 \pm 0.1059$; 9/10 subjects showed significance). For all subjects in the FS task the movement durations were distinctly seen as two clusters (see Fig. 8*A*): one cluster corresponding to a lower movement duration at lower RPTs and another cluster corresponding to a higher movement duration at higher RPTs. A Hartigan's dip test for unimodality showed significance (mean Dip Stats = 0.0895 ± 0.03; 9/10 subjects show significance, $P < 0.001$), indicating that the movement duration of the switch trials in the FS task was indeed not a unimodal distribution. This observation indicated that the subjects exhibited two distinct plans for fast movements and slow movements in the FS task.

In contrast to the FS task, where the movement duration as a function of the RPT was seen as two clusters, the movement duration in the SF task showed a single distribution. The Hartigan's dip test for unimodality did not show significance, indicating that the movement duration distribution was not a bimodal distribution (mean Dip Stats = 0.022 ± 0.0038; 10 subjects, $P > 0.05$), whereas the movement duration of the switch trials in the SF task clearly showed a negative trend as a function of RPT (Pearson's $r = -0.5236 \pm 0.0722$, 9/10 subjects showed significance; see Fig. 8*B*). This result suggests a merging and gradual replacement of one plan over the initial plan as a function of RPT.

Parallel Programming Model for Predicting Movement Duration in the SF Task

The movement duration in switch trials in the SF task followed a negative trend as a function of RPT. This indicates a gradual merging of two movement plans. We quantitatively evaluated a replacement model by weighting the two individual movement plans (i.e., their movement durations) by their respective planning times to assess whether the movement duration trend could be predicted as a function of RPT in the SF task (see *Eqs. 11–13*).

Table 1. *Summary of statistical test results*

Models	Weibull Mean Population Analysis (*t*-test)	KS Test for Individual Subjects for CDF of Weibull Function	Mean RT of Error Response Population Analysis (*t*-test)	KS Test for Individual Subjects for RTs of Erroneous Response
		Fast-to-slow task		
GG independent	$P < 0.001$	$P < 0.05$ (10/10)	$P < 0.001$	$P < 0.05$ (8/10)*
GG symmetric	$P < 0.001$	$P < 0.05$ (10/10)	$P < 0.001$	$P < 0.05$ (10/10)
GG asymmetric	**$P = 0.9155$ $BF_{10} = 0.3104$**	**$P > 0.05$ (9/10)†**	$P < 0.001$	$P < 0.05$ (10/10)
GSG independent	**$P = 0.9675$ $BF_{10} = 0.3091$**	**$P > 0.05$ (10/10)**	**$P = 0.257$ $BF_{10} = 0.5527$**	**$P > 0.05$ (8/10)**
GSG symmetric	$P < 0.05$	$P < 0.05$ (10/10)	$P < 0.05$	$P < 0.05$ (9/10)†
GSG asymmetric	$P < 0.05$	$P < 0.05$ (10/10)	$P < 0.05$	$P < 0.05$ (9/10)†
GSG asymmetric 2	**$P = 0.205$ $BF_{10} = 0.6521$**	**$P > 0.05$ (8/10)***	$P < 0.05$	$P < 0.05$ (10/10)
GS mutually interactive	**$P = 0.267$ $BF_{10} = 0.6485$**	$P > 0.05$ (7/10)‡	$P < 0.05$	$P < 0.05$ (10/10)
		Slow-to-fast task		
GG independent	$P < 0.001$	$P < 0.05$ (10/10)	**$P = 0.4119$ $BF_{10} = 0.4198$**	$P < 0.05$ (8/10)*
GG symmetric	$P < 0.001$	$P < 0.05$ (10/10)	**$P = 0.115$ $BF_{10} = 0.9758$**	$P < 0.05$ (10/10)
GG asymmetric	**$P = 0.7228$ $BF_{10} = 0.3271$**	**$P > 0.05$ (8/10)***	$P < 0.001$	$P < 0.05$ (10/10)
GSG independent	**$P = 0.101$ $BF_{10} = 1.044$**	**$P > 0.05$ (7/10)‡**	$P < 0.01$	$P > 0.05$ (6/10)§
GSG symmetric	$P < 0.05$	$P < 0.05$ (10/10)	$P < 0.05$	$P < 0.05$ (9/10)†
GSG asymmetric	$P < 0.05$	$P < 0.05$ (10/10)	$P < 0.05$	$P < 0.05$ (10/10)
GSG asymmetric 2	**$P = 0.8606$ $BF_{10} = 0.121$**	**$P > 0.05$ (9/10)†**	**$P = 0.8603$ $BF_{10} = 0.3132$**	$P < 0.05$ (7/10)‡
GS mutually interactive	**$P = 0.4503$ $BF_{10} = 0.9874$**	**$P > 0.05$ (9/10)†**	$P < 0.05$	$P < 0.05$ (10/10)

Models were selected on the basis of the statistical test at different levels. Boldface indicates instances when a given test showed no statistical difference between predicted and observed data. KS, Kolmogorov-Smirnov; CDF, cumulative distribution function; RT, reaction time; GG, GO-GO; GSG, GO-STOP-GO; GS, GO-STOP; BF_{10}, Bayes factor. Binomial test (*P* values): §0.1719, ‡0.0547, *0.0107, †0.0001. The larger type size represents the model that satisfied all the statistical criteria to emerge as the best model.

$$w_1 = 1 - w_2 \quad (11)$$

$$w_2 = \mathrm{RPT_{sim}}/\mathrm{RPT_{fast}} \quad (12)$$

$$\mathrm{MD_{step}} = \frac{\left\{w_1 \cdot \left(\mathrm{MD_{slow}}\right) + w_2 \cdot \left(\mathrm{MD_{fast}}\right)\right\}}{k \cdot \left(w_1 + w_2\right)} \quad (13)$$

where w_1, w_2 are the weights and k is a constant that takes values in the range 0.1–2 in steps of 0.1. $\mathrm{MD_{slow}}$ and $\mathrm{MD_{fast}}$ are the average movement duration of the no-switch trials of the SF and FS trials, respectively.

RPT was simulated with a LATER model as mentioned in METHODS. *Equation 13* performs the weighted averaging of the movement duration of the fast trials and slow trials. The simulated movement durations of all the switch trials were compared to the experimental movement duration for each subject. The simulated RTs of the fast no-switch trials in the FS condition were used. Thus, the simulated mean movement duration was highly correlated with the experimental mean movement duration (Fig. 8*C* shows the correlation for all subjects). Nine of ten subjects showed significant correlation, and the mean correlation coefficient was 0.6570 ± 0.0985 (Pearson's *r*; $P < 0.05$ for 9/10 subjects). The slopes of the simulated movement duration as a function of simulated RPT were quantified. Similarly, the slope of the experimental data was also quantified. The mean slope of the experimental data was -0.5311 ± 0.1665, and the mean slope of the simulated data was -0.6865 ± 0.1912 (see correlation in Fig. 8*D*), and they were not significantly different from each other ($t = 0.4853$, df = 9, $P = 0.6390$, $BF_{10} = 0.3414$). Taken together, these simulation results suggest that the weighted averaging model was able to explain the movement duration profiles of the SF task.

DISCUSSION

Recent theories of motor planning suggest that movement initiation can be separated into three parts or phases. The first part is target selection, i.e., determining the location of the object of interest (where); the second part involves specification of movement initiation (when); and the third part involves how movements are to be made and requires specification of movement kinematics and dynamics. All these phases are thought to require implicit decision processes that take time and are thought to contribute to the duration and variation in RT (Wong et al. 2015). In this study, we used a novel approach involving a novel speed redirect task along with a race model framework to study the planning and control of kinematics. In this context, we

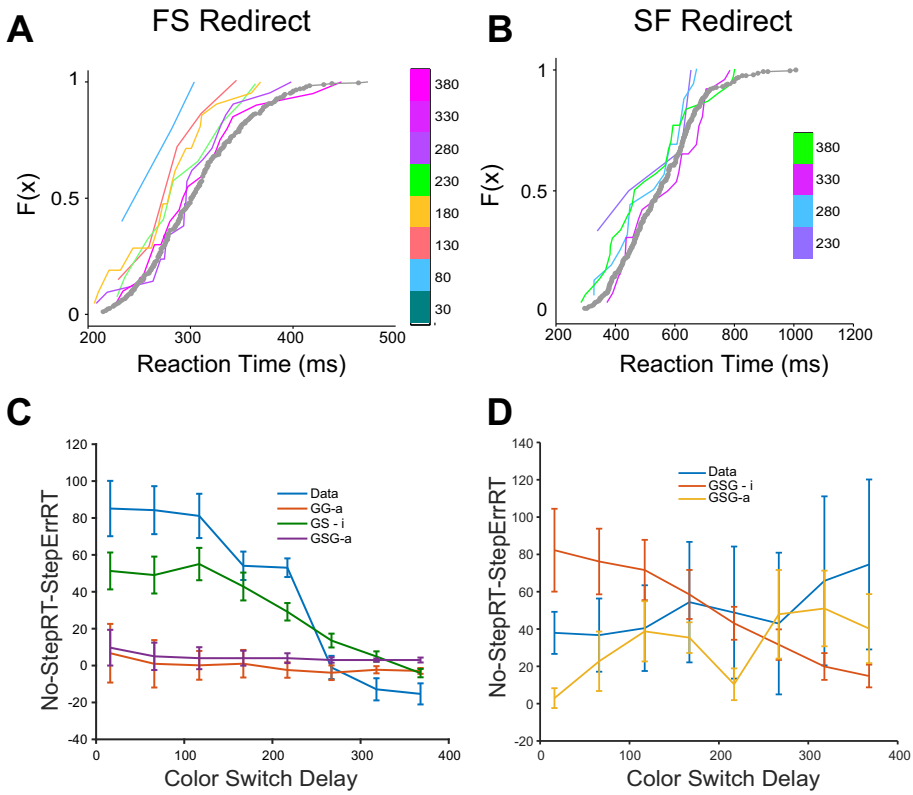

Fig. 7. Testing the fanning effect. *A* and *B*: the fanning effect [F(*x*)] of a single subject in the fast-to-slow (FS) and slow-to-fast (SF) redirect tasks, respectively. The cumulative distributions of erroneous response reaction times (RTs) in switch trials are shown in graded colors for corresponding color switch delays (CSDs), and the no-switch RT distribution is shown in gray. The fanning effect is quantified as the difference between the median no-switch RT and the median RT of the erroneous responses at each CSD. *C* and *D*: quantification of the experimental and simulated conditions for all subjects with each model shown in a different color for FS and SF redirect tasks, respectively. GG-a, GO-GO-asymmetric model; GSG-i, GO-STOP-GO-independent model; GSG-a, GO-STOP-GO-asymmetric model.

investigated various computational architectures underlying the ability to change the speed of movements online.

Performance of Subjects in a Novel Speed Redirect Task

Double-step reach tasks have been limited to studying the change of direction and amplitude. In the present study, we have used a novel speed redirect task in which the position of the target was kept constant while the color of the target was switched, indicating to the subject to change his/her speed of movement. The subjects' performance, as assessed by the compensation function, for FS and SF redirect tasks was qualitatively similar to the performance of the position redirect task from previous studies (Gopal and Murthy 2015, 2016), showing increases in error with CSD. In the present study, movement duration was used interchangeably with speed under the assumption that movement duration directly maps to speed of the movements in the task. However, and interestingly, when the compensation function was computed based on peak or average velocity, the compensation function did not show a strictly monotonically increasing function as obtained based on movement duration. This could be a consequence of using movement duration rather than speed as an online criterion to reward subjects. Although the absence of a strictly monotonic relationship raises the question of whether the duration rather than the speed is a parameter that is explicitly planned and controlled, the monotonically increasing compensation function seen in both SF and FS for movement duration suggests that some aspect of the kinematics is part of the evolving motor plan and justified our use of a race model framework that has explained performance in previous versions of the redirect task in both eye and hand movements (Kapoor and Murthy 2008; Ramakrishnan et al. 2012; Venkataramani et al. 2018).

Testing Race Models

In this study we used a novel speed redirect task and assessed the ability of different race models to predict the performance of subjects. This study is a follow-up of another recently published work (Venkataramani et al. 2018) in which we showed the validity of a similar abort-and-replan independent race model that involved 24 subjects performing a position redirect task. Here we verified the same abort-and-replan model for fast-to-slow changes in speed with similar criteria, suggesting the general applicability of the model when changes in either reach position or speed are required. As in the previous study, we also could not reject some models based on a single criterion, so model selection was based on multiple criteria. These results are summarized in Table 1. For the fast-to-slow condition only the independent GO-STOP-GO model satisfied all the criteria and predicted the fanning effect, while none of the conventional race models explained performance in the FS condition. Thus, relative to all the models tested, the GO-STOP-GO model was taken as the best model to explain the performance for the fast-to-slow condition. While it can be argued that a study with a such a relatively small sample size may not be able to distinguish between alternate hypotheses, here we showed that the same abort-and-replan hypothesis could not explain the performance of the same subjects in the SF condition.

Race Mode Architecture Underlying the FS Condition

GO-GO models. In the position redirect task, the GO-GO class of models clearly failed to explain the behavior and the predictions of the models (Venkataramani et al. 2018). In the present study, fast movements and slow movements represent two distinct plans, and we used the same approach to test the

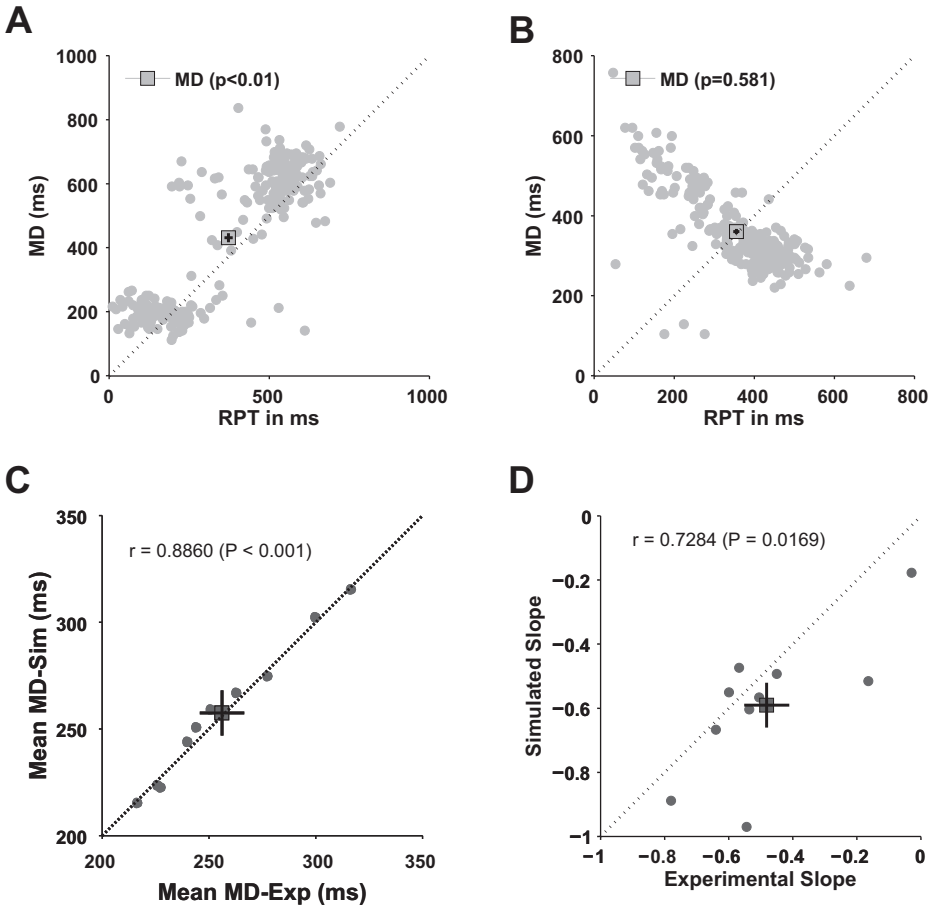

Fig. 8. Relationship between reprocessing time (RPT) and movement duration (MD). *A*: a positive correlation of the MD of the switch trials with RPT in the fast-to-slow (FS) redirect task for an exemplar subject. *B*: a negative correlation of the MD of switch trials with RPT in the slow-to-fast (SF) redirect task for an exemplar subject. *C*: comparison of simulated (Sim) vs. observed (Exp) MDs for all subjects in the SF task. *D*: comparison of simulated vs. observed MD-RPT slopes (from *B*) for all subjects in the SF task. In *C* and *D* each data point is an individual subject.

possibility of GO-GO models to explain performance. Since the fast and slow no-switch trials had distinctly different RTs, the GO processes representing the fast and slow processes were allowed to accumulate at different rates. This reduced GO-GO models to three possible types, namely, GO-GO independent, GO-GO symmetric inhibition, and GO-GO asymmetric inhibition. Models were selected on the basis of their ability to fit the compensation function and predict the error response RTs and fanning effect. The GO-GO independent and GO-GO symmetric inhibition models could not explain the behavior in both FS and SF tasks. This result is expected in the case of the FS condition because the GO1 representing the fast plan has a faster rate and the second GO2 process representing the slow plan, having a slower rate, would always fail to take over the first GO1 process and hence could not explain the behavior. However, when one carefully looks at the predicted compensation function, even at the lowest CSD the probability of the correct response was ~0.5. This result is similar to the position redirect task (Gopal and Murthy 2015), and hence it is reasoned that the rate of accumulation of the GO processes might not influence behavior. The symmetric mutual inhibition model, in which the inhibitory interaction between the two GO processes is mutual, also failed to explain the compensation function for the FS task. This result is because of the fact that in a mutually inhibitory interaction the first GO unit has an advantage inhibiting the weaker second GO2 process rather than the other way. As a result, more of the GO1 units hit the threshold, resulting in a movement toward the first target. To overcome this caveat of the symmetric inhibition model, an asymmetric mutual inhibitory model was tested. The inhibitory interaction coefficient β_{GO2} was found to be more than the β_{GO1}, which compensated for the weaker GO2, inhibiting the stronger GO1 process. This model predicted the compensation function better than the other GO-GO models. Since the β_{GO2} was stronger, the error response RTs predicted by the model were much larger compared with the experimental values. Although a higher coefficient of interaction helped to predict the compensation function, it delayed the GO2 in error responses and hence did not entirely explain the behavior of subjects.

GO-STOP models. In the FS condition, the GO-STOP-GO independent model and the asymmetric model with a free β_{GO1} were able to better predict the compensation function compared with the other models. However, only the independent race model predicted the error response correctly in the FS condition (the fanning effect). Thus only the GO-STOP-GO independent model fitted the data well in terms of behavior, error response, and the fanning effect. This result validates the existence of a STOP process and the independent assumption of the race model. This result is in contrast to previous studies of saccade redirection in which interactive models appear to also explain the data. Although the reasons for these differences are not clear, it is important to note that gaze control is commonly thought to require an active process mediated by fixation neurons that inhibit gaze movement commands during gaze holding. The necessity for an analogous reach fixation system remains unclear, given the high inertial properties of the arm.

Although not obvious, the success of the GO-STOP-GO independent model could be also a consequence of the fast-to-slow change directly mapping onto the STOP process, unlike in the SF task, in which the change of plan involves an increase in speed. In addition, the default pattern of recruitment of muscle fibers may also play a role in the observed differences between SF and FS behaviors. This can also explain why FS may require a complete abortion of a motor plan, while SF could occur with a replacement. According to Henneman's size principle the low-force, fatigue-resistant muscle fibers are recruited before high-force, less fatigue-resistant muscle fibers (McPhedran et al. 1965). In the first case of fast-to-slow transition, the high-force motor units may be recruited as part of the initial movement plan. It has been reported that in a reactive stoppinglike scenario, like the present paradigm (fast to slow), stopping has global effects on the motor system (Aron 2011; Badry et al. 2009). Hence, when the change of plan involves the slowing of movements, the high-force motor units that were recruited would have to be inhibited. However, when subjects are asked to increase their movement speed, the high-force units that are generally recruited later can be co-opted into the evolving movement plan, allowing the SF switch to ride on the natural recruitment principle and increase the movement speed. This could involve gradual replacement of the new motor plan without the need for an explicit STOP signal. According to this hypothesis, the asymmetry is not due to differential recruitment of the slow motor units in the two tasks but a consequence of the "larger" motor units differentially recruited in the fast speed (large force) condition compared with the slow speed (small force) condition. Thus switch trials that demand a change from fast to slow speeds will necessarily require cancelling the plan since the larger motor units would be called into play and would need to be inhibited, whereas changing a plan from slow to fast speeds would only require recruiting the additional larger motor units to produce the faster speeds. This notion may explain why none of the race models could explain the SF task results.

Computational Mechanisms Underlying the SF Condition

Unlike the FS task, none of the race models was able to satisfactorily explain the performance of subjects in the SF task. Although the independent model produced accurate compensation function, it could not predict the error response RTs in the SF task. This is because the experimental data of the SF condition did not show a fanning effect, violating the independence assumption. As alluded to above, unlike in the FS task, where there is slowing of intended movement, the SF task requires a speeding up of movement and the mechanism of stopping a response, and thus it does not easily map onto such a requirement. The modeling results clearly reflect this asymmetry and reflect why the model that best fit the FS data required inhibition while none of the GO-GO or GO-STOP models was able to explain the SF data.

The failure of race models was not just quantitative in nature but was qualitative, too. This is supported by the observation that the movement duration of the switch trials as a function of RPT in the SF task showed a gradual change from slow to fast. On the other hand, the FS task distinctly showed two distributions of movement duration in switch trials, supporting the notion that fast and slow movements were distinctly separated when the switching movement plan from fast to slow happened. The observation of such a distinction further reinforces the validity of the online and off-line criteria used to distinguish slow movements (>500 ms and <1,000 ms) from fast movements (<200 ms), allowing us to differentiate incorrect and correct switch trials in the FS condition but not in the SF condition. Interestingly, a weighted averaging model could predict the gradually changing speed plans in the SF task. The use of this model was motivated by earlier studies (Aslin and Shea 1987; Becker and Jürgens 1979; Bhutani et al. 2012) that used the gradual change of saccadic end points as a function of time delay (D, equivalent to RPT in the present study) in a double-step task (amplitude change) as a proxy for parallel programming. In this context, Becker and Jürgens (1979) proposed that the internal representation of target location gradually shifts along the straight line connecting the first and second target locations. Furthermore, they assumed that the stimulus was continuously sampled for a fixed period after its presentation. If the target shifts during this time window, a weighted average of two target locations would be specified as the first target location. If the delay between the two stimuli is shorter, the weighted average would be closer to the final target position. Recent efforts have been made to predict the saccade end points as a function of RPT with such an averaging model (Bhutani et al. 2017). In a similar vein, in the context of the present study, the two competing representations could be considered as the two speed plans merging together. This model was able to explain the gradual change of the movement duration as a function of RPT. These results indicate the existence of a kinematic plan of speed and the gradual merging of two such plans in the SF task.

GRANTS

This study was supported by grants from the Department of Science and Technology (IRHPA), Government of India, and a DBT-IISc partnership program grant. P. V. Venkataratamani was supported by a fellowship from the Indian Institute of Science.

DISCLOSURES

No conflicts of interest, financial or otherwise, are declared by the authors.

AUTHOR CONTRIBUTIONS

P.V.V. and A.M. conceived and designed research; P.V.V. performed experiments; P.V.V. analyzed data; P.V.V. and A.M. interpreted results of experiments; P.V.V. prepared figures; P.V.V. drafted manuscript; P.V.V. and A.M. edited and revised manuscript; P.V.V. and A.M. approved final version of manuscript.

REFERENCES

Aron AR. From reactive to proactive and selective control: developing a richer model for stopping inappropriate responses. *Biol Psychiatry* 69: e55–e68, 2011. doi:10.1016/j.biopsych.2010.07.024.

Aslin RN, Shea SL. The amplitude and angle of saccades to double-step target displacements. *Vision Res* 27: 1925–1942, 1987. doi:10.1016/0042-6989(87)90058-7.

Badry R, Mima T, Aso T, Nakatsuka M, Abe M, Fathi D, Foly N, Nagiub H, Nagamine T, Fukuyama H. Suppression of human cortico-motoneuronal excitability during the Stop-signal task. *Clin Neurophysiol* 120: 1717–1723, 2009. doi:10.1016/j.clinph.2009.06.027.

Becker W, Jürgens R. An analysis of the saccadic system by means of double step stimuli. *Vision Res* 19: 967–983, 1979. doi:10.1016/0042-6989(79)90222-0.

Bhutani N, Ray S, Murthy A. Is saccade averaging determined by visual processing or movement planning? *J Neurophysiol* 108: 3161–3171, 2012. doi:10.1152/jn.00344.2012.

Bhutani N, Sengupta S, Basu D, Prabhu NG, Murthy A. Parallel activation of prospective motor plans during visually-guided sequential saccades. *Eur J Neurosci* 45: 631–642, 2017. doi:10.1111/ejn.13496.

Boucher L, Palmeri TJ, Logan GD, Schall JD. Inhibitory control in mind and brain: an interactive race model of countermanding saccades. *Psychol Rev* 114: 376–397, 2007. doi:10.1037/0033-295X.114.2.376.

Carpenter RH, Williams ML. Neural computation of log likelihood in control of saccadic eye movements. *Nature* 377: 59–62, 1995. doi:10.1038/377059a0.

Churchland MM, Santhanam G, Shenoy KV. Preparatory activity in premotor and motor cortex reflects the speed of the upcoming reach. *J Neurophysiol* 96: 3130–3146, 2006. doi:10.1152/jn.00307.2006.

Cisek P. Preparing for speed. Focus on "Preparatory activity in premotor and motor cortex reflects the speed of the upcoming reach". *J Neurophysiol* 96: 2842–2843, 2006. doi:10.1152/jn.00857.2006.

Desmurget M, Grafton S. Forward modeling allows feedback control for fast reaching movements. *Trends Cogn Sci* 4: 423–431, 2000. doi:10.1016/S1364-6613(00)01537-0.

Desmurget M, Grafton S. Feedback or feedforward control: end of a dichotomy. In: *Taking Action: Cognitive Neuroscience Perspectives on Intentional Acts*, edited by Johnson-Frey SH. Cambridge, MA: MIT Press, 2003, p. 289–338.

Dick JP, Benecke R, Rothwell JC, Day BL, Marsden CD. Simple and complex movements in a patient with infarction of the right supplementary motor area. *Mov Disord* 1: 255–266, 1986. doi:10.1002/mds.870010405.

Flanagan JR, Nakano E, Imamizu H, Osu R, Yoshioka T, Kawato M. Composition and decomposition of internal models in motor learning under altered kinematic and dynamic environments. *J Neurosci* 19: RC34, 1999. doi:10.1523/JNEUROSCI.19-20-j0005.1999.

Gopal A, Murthy A. Eye-hand coordination during a double-step task: evidence for a common stochastic accumulator. *J Neurophysiol* 114: 1438–1454, 2015. doi:10.1152/jn.00276.2015.

Gopal A, Murthy A. A common control signal and a ballistic stage can explain the control of coordinated eye-hand movements. *J Neurophysiol* 115: 2470–2484, 2016. doi:10.1152/jn.00910.2015.

Hanes DP, Carpenter RH. Countermanding saccades in humans. *Vision Res* 39: 2777–2791, 1999. doi:10.1016/S0042-6989(99)00011-5.

Hanes DP, Schall JD. Neural control of voluntary movement initiation. *Science* 274: 427–430, 1996. doi:10.1126/science.274.5286.427.

Jana S, Gopal A, Murthy A. Evidence of common and separate eye and hand accumulators underlying flexible eye-hand coordination. *J Neurophysiol* 117: 348–364, 2017. doi:10.1152/jn.00688.2016.

Kapoor V, Murthy A. Covert inhibition potentiates online control in a double-step task. *J Vis* 8: 20, 2008. doi:10.1167/8.1.20.

Keele S. Movement control in skilled motor performance. *Psychol Bull* 70: 387–403, 1968. doi:10.1037/h0026739.

Krakauer JW, Ghilardi MF, Ghez C. Independent learning of internal models for kinematic and dynamic control of reaching. *Nat Neurosci* 2: 1026–1031, 1999. doi:10.1038/14826.

McPhedran AM, Wuerker RB, Henneman E. Properties of motor units in a homogeneous red muscle (soleus) of the cat. *J Neurophysiol* 28: 71–84, 1965. doi:10.1152/jn.1965.28.1.71.

Moran DW, Schwartz AB. Motor cortical representation of speed and direction during reaching. *J Neurophysiol* 82: 2676–2692, 1999. doi:10.1152/jn.1999.82.5.2676.

Morris ME, Summers JJ, Matyas TA, Iansek R. Current status of the motor program. *Phys Ther* 74: 738–748, 1994. doi:10.1093/ptj/74.8.738.

Oldfield RC. The assessment and analysis of handedness: the Edinburgh inventory. *Neuropsychologia* 9: 97–113, 1971. doi:10.1016/0028-3932(71)90067-4.

Padoa-Schioppa C, Li CS, Bizzi E. Neuronal correlates of kinematics-to-dynamics transformation in the supplementary motor area. *Neuron* 36: 751–765, 2002. doi:10.1016/S0896-6273(02)01028-0.

Ramakrishnan A, Chokhandre S, Murthy A. Voluntary control of multi-saccade gaze shifts during movement preparation and execution. *J Neurophysiol* 103: 2400–2416, 2010. doi:10.1152/jn.00843.2009.

Ramakrishnan A, Sureshbabu R, Murthy A. Understanding how the brain changes its mind: microstimulation in the macaque frontal eye field reveals how saccade plans are changed. *J Neurosci* 32: 4457–4472, 2012. doi:10.1523/JNEUROSCI.3668-11.2012.

Reddi BA, Carpenter RH. The influence of urgency on decision time. *Nat Neurosci* 3: 827–830, 2000. doi:10.1038/77739.

Reddi BA, Asrress KN, Carpenter RH. Accuracy, information, and response time in a saccadic decision task. *J Neurophysiol* 90: 3538–3546, 2003. doi:10.1152/jn.00689.2002.

Rosenbaum DA. Motor programming: a review and scheduling theory. In: *Motor Behavior: Programming, Control, and Acquisition*, edited by Heuer H, Kleinbeck U, Schmidt KH. Berlin: Springer, 1985, p. 1–33. doi:10.1007/978-3-642-69749-4_1.

Scott SH. Optimal feedback control and the neural basis of volitional motor control. *Nat Rev Neurosci* 5: 532–546, 2004. doi:10.1038/nrn1427.

Shadmehr R, Mussa-Ivaldi FA. Adaptive representation of dynamics during learning of a motor task. *J Neurosci* 14: 3208–3224, 1994. doi:10.1523/JNEUROSCI.14-05-03208.1994.

Summers JJ, Anson JG. Current status of the motor program: revisited. *Hum Mov Sci* 28: 566–577, 2009. doi:10.1016/j.humov.2009.01.002.

Todorov E, Jordan MI. Optimal feedback control as a theory of motor coordination. *Nat Neurosci* 5: 1226–1235, 2002. doi:10.1038/nn963.

Usher M, McClelland JL. The time course of perceptual choice: the leaky, competing accumulator model. *Psychol Rev* 108: 550–592, 2001. doi:10.1037/0033-295X.108.3.550.

Venkataramani P, Gopal A, Murthy A. An independent race model involving an abort and re-plan strategy explains reach redirecting movements during planning and execution. *Eur J Neurosci* 47: 460–478, 2018. doi:10.1111/ejn.13821.

Wolpert DM, Ghahramani Z. Computational principles of movement neuroscience. *Nat Neurosci* 3, *Suppl*: 1212–1217, 2000. doi:10.1038/81497.

Wolpert DM, Ghahramani Z, Jordan MI. An internal model for sensorimotor integration. *Science* 269: 1880–1882, 1995. doi:10.1126/science.7569931.

Wolpert DM, Kawato M. Multiple paired forward and inverse models for motor control. *Neural Netw* 11: 1317–1329, 1998. doi:10.1016/S0893-6080(98)00066-5.

Wong AL, Haith AM, Krakauer JW. Motor Planning. *Neuroscientist* 21: 385–398, 2015. doi:10.1177/1073858414541484.